## Effect of Ion Identity on Capacitance and Ion-to-Electron

## Transduction in Ion-Selective Electrodes with Nanographite and

### **Carbon Nanotube Solid Contacts**

Celeste R. Rousseau, Yevedzo E. Chipangura, Andreas Stein, and Philippe Bühlmann\*

Department of Chemistry, University of Minnesota, 207 Pleasant St. SE, Minneapolis MN 55455, USA

\*Corresponding author

#### Abstract

The use of large surface-area carbon materials as transducers in solid-contact ion-selective electrodes (ISEs) has become widespread. Desirable qualities of ISEs, such as small long-term drift, have been associated with a high capacitance that arises from the formation of an electrical double layer at the interface of the large surface-area carbon material and the ion-selective membrane. The capacitive properties of these ISEs have been observed using a variety of techniques, but effects of the ions present in the ion-selective membrane on the measured value of the capacitance have not been studied in detail. Here, it is shown that changes in the size and concentration of the ions in the ion-selective membrane as well as the polarity of the polymeric matrix result in capacitances that can vary by up to several hundred percent. This data illustrates that the interpretation of comparatively small differences in capacitance for different types of solid contacts is not meaningful unless the composition of the ion-selective membrane is taken into account.

#### Introduction

Over the past 30 years, much research on ISEs focused on new solid contact materials, eliminating the inner filling solutions of conventional setups. 1-5 Important advantages of solid-contact ISEs are easier maintenance and reduction of pressure sensitivity, expanding the range of possible applications. The primary function of the solid contact material contacting the ion-conducting sensing membrane is to act as ion-to-electron transducer. Conducting polymers, 6-14 redox-active organometallic complexes and redox buffers, 15-17 as well as intercalation compounds have been studied extensively as transducers for solid-contact ISEs, as have redox-inactive materials with large surface areas. Among the latter, carbon materials have been studied the most, such as three-dimensionally ordered macroporous (3DOM) carbon, 19-20 colloid-imprinted mesoporous (CIM) carbon, 21-22 single-walled carbon nanotubes (SWCNTs), 23-24 multi-walled carbon nanotubes (MWCNTs), 25-28 graphene, 29-30 reduced graphene oxide, 31-32 carbon black, 33-34 fullerene, 35 carbon nanospheres, 36 carbon nanohorns, 37 and carbon cloth. 38

The transduction mechanism of non-redox active transducers has been established as arising from a large double-layer capacitance at the interface between the solid-contact material and the ISE membrane, as shown, e.g., by studies on sensors with 3DOM carbon solid contacts.<sup>20</sup> The magnitude of the capacitance depends on the surface chemistry and surface area of the carbon.<sup>20</sup> A capacitive transduction mechanism was also confirmed for sensors with SWCNTs<sup>39</sup> and reduced graphene oxide<sup>31</sup> solid contacts.

A variety of electrochemical techniques can be used to determine the capacitance of a solid contact, including chronopotentiometry,<sup>9</sup> electrochemical impedance spectroscopy (EIS),<sup>40-42</sup> and cyclic voltammetry (CV).<sup>20</sup> When studying fully assembled sensors, chronopotentiometry is preferable to other techniques, as data interpretation is more straightforward and the high

resistance of the ion-selective membrane does not affect the data as much as for EIS<sup>40</sup> and CV. Chronopotentiometry to measure the low-frequency capacitance of ISE solid contacts was introduced by Bobacka, <sup>9</sup> initially to study conducting polymer-based transducers, but has subsequently been used widely for capacitive high-surface area solid contacts too. <sup>21, 24, 43</sup> The potential change over time as measured in chronopotentiometry allows the capacitance of a sensor to be calculated, with smaller derivatives in the potential versus time plots corresponding to higher capacitances. <sup>9</sup> High capacitances associated with high surface area carbon materials generally correspond to low potential drifts in long-term potentiometric ion sensing, with some transducers displaying drifts  $\leq$ 10  $\mu$ V/h. <sup>21, 31, 33</sup> We note, however, that although a high capacitance is important for long-term stability of the measured potential under otherwise ideal conditions, other features of the sensors can affect observed potential stabilities, such as the hydrophobicity of ionic sites and ionophores, the stability of ionophore complexes, and the underlying electrode material. <sup>4, 44-46</sup>

Recently, the protocol for chronopotentiometric capacitance measurements was investigated thoroughly for ISEs with octadecylamine-modified SWCNTs as solid contacts. It was found that use of several current magnitudes and multiple cycles of positive and negative currents improves the reliability of measurements. The same study also compared capacitances before and after deposition of ion-selective membranes onto the SWCNTs, showing that the capacitance changed little for ionophore-free NO<sub>3</sub><sup>-</sup> exchanger membranes, but decreased 30% to 50% for ionophore-based K<sup>+</sup> and Ca<sup>2+</sup> sensors. These observations critically improved the methodology to characterize capacitive solid contacts.

To determine whether the identity and size of the ions in the ion-selective membrane affect device capacitance significantly, we compare here directly capacitances of sensing

membranes that comprised different ions. Effects of the plasticizer and ion concentration were also studied. The dependence of the capacitance on these factors was overlooked in the past, and small differences in the capacitances of devices with different solid-contact materials were emphasized, without taking differences in the composition of the ion-selective membranes into account. This work helps to assess how meaningful such comparisons are. To illustrate effects of several different parameters, this work used many combinations of solid contact materials, types of ionic sites, ionic site concentrations, and target ions. Readers may find Table S1 useful, which shows a list of all the systems for which capacitance was assessed in this work.

### **Experimental Methods**

Nanographite powder (GS-4827) was purchased from Graphite Store<sup>47</sup> (Northbrook, IL, USA). A suspension of 50 mg of nanographite in 1 mL of THF was sonicated for  $\geq$  30 min, and 4  $\mu$ L of this suspension was drop-cast onto a gold or glassy carbon electrode, followed by deposition of the ion-selective membrane. For details on other experimental details, see the Supporting Information.

#### **Results and Discussion**

Theory of Double Layer Capacitance at Varying Electrode Potential

According to the Gouy–Chapman–Stern model, the electrical double layer at an electrode surface comprises a closely packed Stern layer at the electrode surface and a diffuse layer that extends away from the electrode surface into the solution. This is consistent with the occurrence of a potential of zero charge (PZC), and it predicts that the double layer capacitance increases as the potential deviates from the PZC and ions are packed more closely. However, as a result of their non-zero size, ions cannot pack infinitely tightly, and the value of the capacitance

levels off at potentials farther from the PZC and decreases at even more extreme potentials.<sup>49-51</sup>
Larger ions result in a smaller capacitance, as fewer ions are able to pack within the same space.

To take into account ion size, the Gouy–Chapman–Stern theory can be extended using a modified Poisson–Boltzmann model,<sup>51-52</sup> which describes the capacitance of the diffuse layer as follows:

$$C_d = \frac{2zeN_A c_{\text{bulk}} \lambda_D}{\psi_D} \sqrt{\frac{2}{\nu} \log\left[1 + 2\nu \sinh^2\left(\frac{ze\psi_D}{2k_B T}\right)\right]}$$
(4.1)

where z is ionic charge (for a symmetrical electrolyte with  $z = z_{\text{cation}} = -z_{\text{anion}}$ ), e is the elementary charge,  $N_A$  is Avogadro's number,  $c_{\text{bulk}}$  is the electrolyte concentration in the bulk of the solution,  $\lambda_D$  is the Debye length,  $\psi_D$  is the potential of the electrode surface relative to the PZC,  $k_B$  is the Boltzmann constant, and T is the absolute temperature. Ion size is taken into account with  $\nu$ , a packing parameter calculated using

$$v = 2a^3 N_A c_{\text{bulk}} \tag{4.2}$$

where *a* is the effective ion diameter. A drawback of this model is that it assumes cations and anions to have the same size. Therefore, modifications of this theory for systems with asymmetrically sized ions were reported.<sup>53-54</sup>

The approach used here applies mean field theory to model the diffuse layer capacitance and describes the solution in terms of the number of sites available to ions, the number of ions present, and the relative cation and anion sizes (for details, see the Supporting Information).<sup>53</sup>

Predictions of the double layer capacitance using this modified model are shown in Figure 1. The five electrolyte compositions shown in this graph correspond to the systems studied experimentally in this work.

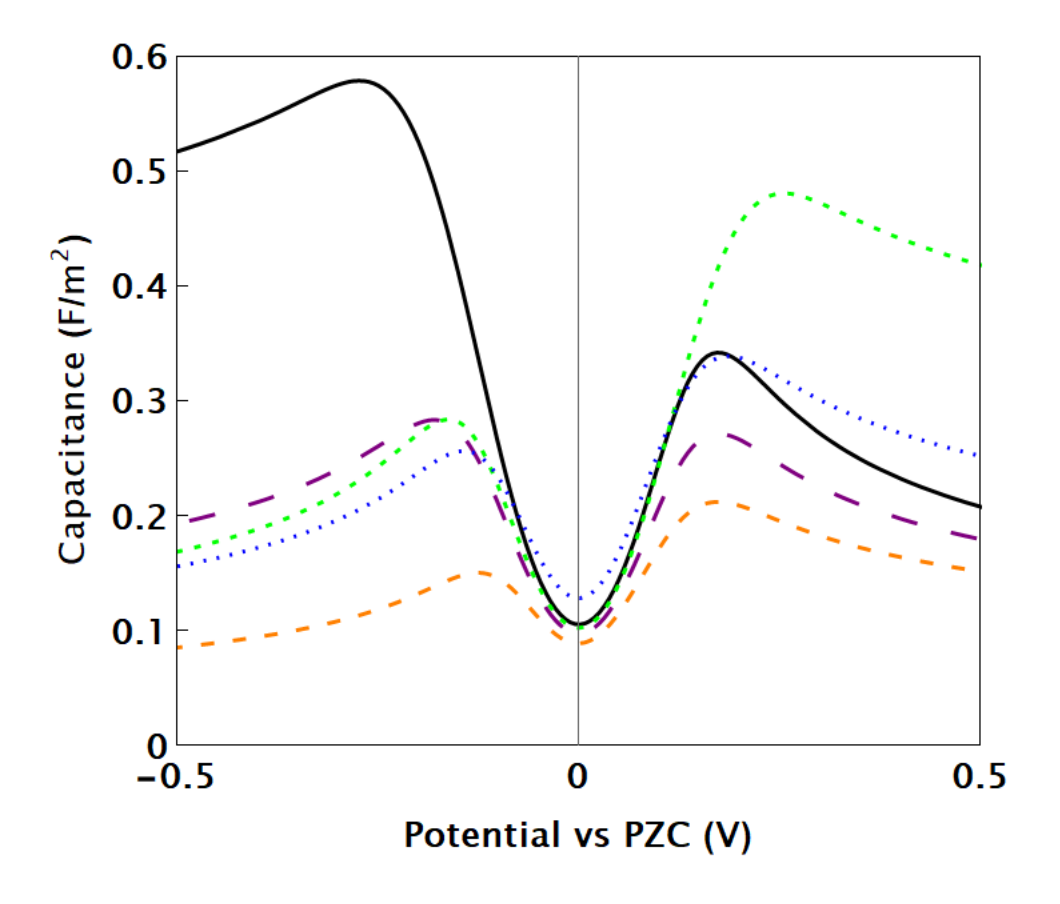


Figure 1. Predictions from mean-field modification of the Gouy–Chapman–Stern model for the double-layer capacitance of the following electrolyte solutions (on the left, top to bottom): potassium tetrakis(perfluorophenyl)borate (K·TPFPB; black), tetrabutylammonium tetrakis(perfluorophenyl)borate (TBA·TPFPB; purple, long dashed), tridodecylmethylammonium nitrate (TDDMA·NO3; green, short dashed), TDDMA·NO3 + tetradodecylammonium tetrakis(4-chlorophenyl)borate (ETH500; blue, dotted), and [K+valinomycin]·TPFPB (orange, medium dashed). Potentials are referenced for each individual system to the PZC. For the dielectric constant as well as cation and anion sizes and concentrations used to calculate capacitances in this manner, see the Supporting Information.

As Figure 1 illustrates, a key prediction of this model is that, in spite of adjustments for asymmetric ion size, the capacitance near the PZC is only affected to a small extent by the size

of ions present. Further away from the PZC, ion size matters more. Moreover, addition of an electrolyte is predicted to result in an increase in capacitance, even at the PZC, as an increased ion concentration decreases the Debye length.

Yet, it is important to note that the PZC is not easily defined for electrodes that are not single crystals. Different crystal facets exposed on the electrode surface will have different PZCs, <sup>48</sup> and amorphous electrode materials do not have a well-defined PZC. Moreover, specific adsorption of ions to the electrode alters the PZC, causing it to deviate from the potential at which the capacitance is smallest. <sup>55</sup> Specific adsorption can be driven by favorable interactions between the adsorbed ions and the electrode material, such as between chloride and gold electrodes, but it can also be the result of solvophobic effects, resulting in surface activity and, possibly, the preferential alignment of ions at the electrode surface. This has been shown to occur for ionic sites and ionophore complexes used to induce permselectivity and control the selectivity of ISE membranes, where the polar groups of these species effectively gather at the membrane/water interface. <sup>56-58</sup> Similar effects may also occur at the surface of carbon transducers. One of the few examples to date for this is the depletion of the K<sup>+</sup> ionophore BME-44 from ion-selective membranes in contact with colloid-imprinted mesoporous carbon. <sup>59</sup>

As illustrated by Figure S2, the capacitance is also affected by the dielectric constant. The capacitance of ISE membranes plasticized with bis(2-ethylhexyl) sebacate (DOS;  $\varepsilon$ =3.9)<sup>60</sup> is predicted to be significantly smaller at the PZC and all other potentials than for membranes plasticized with *o*-nitrophenyl octyl ether (*o*-NPOE,  $\varepsilon$ =23.9).<sup>60</sup>

#### Nanographite

In order to measure the effects of ion identity on capacitance with an easily available, low-cost, high surface area carbon material, we used in this work a nanographite powder

previously utilized as solid-contact material for ISEs.<sup>61-62</sup> Nanographite is composed of graphite platelets with a particle size distribution from 0.10 to 10 μm.<sup>47</sup> It has a Brunauer–Emmett–Teller (BET) surface area of 165 m²/g, comparable to three other carbon transducers recently used very effectively, i.e., 3DOM carbon (247 m²/g),<sup>20</sup> CIM carbon (442 m²/g),<sup>21</sup> and SWCNTs (124 to 1024 m²/g, depending on the preparation and manufacturer).<sup>63</sup> Approximately one quarter of the surface area arises from micropores (<2 nm), the remainder from mesopores (2–50 nm) and a small fraction (~2%) from the external surfaces. For the nitrogen sorption isotherm, see the Supporting Information, Figure S1.

Capacitance of Glassy Carbon Electrodes and High Surface Area Carbons in Absence of Ion-Selective Membranes

The capacitance of bare glassy carbon electrodes in absence of an ion-selective membrane was measured first, using o-NPOE solutions of ionic site salts commonly used in ionophore-free ion-exchanger ISEs. EIS spectra could be measured (see Figures S3 and S4) because the overall resistances of o-NPOE solutions without a polymer component are relatively low. The capacitances of the bare glassy carbon electrodes in 10 mM Li·TPFPB and 10 mM TDDMA·Cl solutions were found to be within error identical ( $6.2\pm0.7~\mu\text{F}$  or  $87\pm10~\mu\text{F/cm}^2$ ; and  $5.9\pm0.9~\mu\text{F}$  or  $83\pm13~\mu\text{F/cm}^2$ , respectively; N=3), in spite of the very different sizes of the cation and anion in these solutions. Notably, there was within error no effect on the measured capacitance when a DC bias potential in the range of -100~mV to +100~mV relative to the open circuit potential (OCP) was applied to the glassy carbon electrode (see Table S2).

The capacitances of both nanographite- and SWCNT-modified glassy carbon electrodes were studied as representative high-surface-area carbon solid contacts, also using 10 mM solutions of Li·TPFPB or TDDMA·Cl in *o*-NPOE in the range from -100 to +100 mV versus the

OCP. Not surprisingly, the capacitances of all electrodes modified with nanographite or SWCNTs were approximately three orders of magnitude larger than for bare glassy carbon (see Tables S2 and S3).

For electrodes coated with SWCNTs, the average capacitance in Li·TPFPB was  $6.1 \pm 0.7$  mF, while in TDDMA·Cl the average capacitance was  $4.9 \pm 0.8$  mF. Within error, the identity of the electrolyte ions does not have a measurable effect on the capacitance. This is consistent with the theory of double-layer capacitance discussed above, which predicts the ion size effect near the PZC to be small. Notably, the capacitance of SWCNT electrodes in o-NPOE solutions is quite repeatable from electrode to electrode. This is due in part to the comparatively robust films that are formed with SWCNTs, which are not disturbed by immersion into the electrolyte solution.

Conversely, the nanographite does not form a very robust film, even when poly(vinyl chloride) (PVC) is included as a binder in a 1:9 ratio w/w with respect to the nanographite. Notwithstanding, even though there is electrode-to-electrode variability in the magnitude of the capacitance (see Figure S5), the capacitance of the nanographite films was affected for each electrode in the same way by the application of a DC potential bias (see Table S3). In solutions of Li·TPFPB, the measured capacitance was higher at negative potentials than at the OCP, while in solutions of TDDMA·Cl, the measured capacitance was higher at positive potentials than at the OCP. This suggests that the capacitance is higher at potentials where the smaller ion has a higher concentration near the surface.

In contrast, with SWCNT electrodes (see Figure S6 and Table S4), there does not appear to be any effect of the potential on capacitance in Li·TPFPB solutions. Notably, in solutions of TDDMA·Cl, SWCNT electrodes show an unexpected effect at positive potentials. When the DC

bias potential was applied for 10 min prior to acquisition of the EIS spectra, the observed current was much higher than in the case of Li·TPFPB solutions, suggesting occurrence of an electrochemical reaction taking place at the SWCNT surface.

Effects of Ion Identity and Ion Concentration on Double-layer Capacitance of ISEs with Ion-Selective Membranes

Nanographite solid-contact ISEs with ion-selective membranes comprising PVC, *o*-NPOE, and one of several salts were studied. The latter were tridodecylmethylammonium nitrate (TDDMA·NO<sub>3</sub>), tetrabutylammonium tetrakis(pentafluorophenyl)borate (TBA·TPFPB), or potassium tetrakis(pentafluorophenyl)borate (K·TPFPB) to provide for ion exchanger sites. In the case of K·TPFPB, experiments were also performed with an additional 200 mol % valinomycin as K<sup>+</sup> binding ionophore. These salts were chosen to include both an example of a large anion together with a small cation (TBA·TPFPB) and examples of a large cation paired with a smaller anion (TDDMA·NO<sub>3</sub>; [K+valinomycin]·TPFPB), as well as two ions of similar size (TBA·TPFPB). Relevant ionic radii are listed in Table S5. The capacitances of the respective ISEs were measured using chronopotentiometry by applying currents of several magnitudes, with 8 cycles of positive and negative currents periods of 2×10 s each.

Table 1 details the capacitances calculated from chronopotentiograms with  $\pm 50$  nA,  $\pm 100$  nA, and  $\pm 500$  nA currents (for examples of chronopotentiograms, see Figure S7). For the smaller currents, the interface of the sensing membrane and the nanographite is charged only minimally over the 10 s during which a current is applied, and the measured potential does not change by more than  $\sim 10$  mV on application of  $\pm 50$  nA. Under these circumstances, the measured capacitance does not have a significant dependence on the magnitude and direction of the applied

current (although, for membranes doped with TDDMA·NO<sub>3</sub>, there appears to be some effect on the direction of applied current at a magnitude of  $\pm$  500 nA).

**Table 1.** Capacitance at ±500, ±100, and ±50 nA current magnitudes for electrodes with nanographite solid contacts and *o*-NPOE-plasticized PVC membranes containing K·TPFPB, TBA·TPFPB, TDDMA·NO<sub>3</sub>, or [K+valinomycin]·TPFPB. In most cases, the capacitance is not affected by the direction of the current.

current (nA)	capacitance (mF)	specific capacitance (F/g) <sup>a</sup>
K·TPFPB <sup>b</sup>		
±500	1.02±0.10	5.1±0.5
±100	$1.04\pm0.11$	5.2±0.6
±50	1.03±0.16	5.2±0.8
$TBA \cdot TPFPB^{\ b}$		
±500	$0.59\pm0.04$	3.0±0.2
±100	$0.59\pm0.05$	$3.0\pm0.3$
±50	0.59±0.06	$3.0\pm0.3$
$TDDMA\cdot NO_3^{\ b}$		
±500	$0.35 \pm 0.07$	1.8±0.4
±100	$0.34 \pm 0.04$	1.7±0.2
±50	$0.36 \pm 0.04$	$1.8 \pm 0.2$
$K \cdot TPFPB^b + valinomycin^c$		
±500	$0.24 \pm 0.03$	1.2±0.2
±100	$0.23 \pm 0.03$	1.2±0.2
±50	$0.25 \pm 0.03$	1.3±0.2

<sup>&</sup>lt;sup>a</sup> Capacitance per g of nanographite <sup>b</sup> 10 mmol/kg <sup>c</sup> 20 mmol/kg in total; 10 mmol/kg as [K+valinomycin]<sup>+</sup> complex and 10 mmol/kg as free ionophore.

As Table 1 shows, for a set of electrodes prepared on the same day with the same nanographite suspension, the capacitance depends on the identity of the ions in the membrane. Specifically, the overall capacitance was found to be 75% and 329% larger for electrodes with K·TPFPB doped membranes than when the membranes contained the same anion (TPFPB<sup>-</sup>) but either tetrabutylammonium or the K<sup>+</sup> complex of valinomycin, respectively, as the cation. This shows that changing the identity of just one of the ions can significantly affect the capacitance. The capacitance of electrodes with TDDMA·NO<sub>3</sub> membranes fell in between those of ISEs with either TBA·TPFPB or [K+valinomycin]·TPFPB. This demonstrates that the overall capacitance is indeed affected substantially by ion size. Notably, the capacitance per weight of solid contact material decreases significantly with the addition of the ion-selective membrane, as expected. Apart from effects related to other components of the membrane, it is likely that the presence of PVC not only lowers the membrane polarity but also reduces the carbon surface area that is accessible to ions, and that this contributes to some extent to the reduced capacitance.

Notably, we found a significant batch-to-batch variability in capacitance of electrodes with nanographite solid contacts in spite of painstaking efforts to standardize all fabrication steps. This may be caused by differences in the nature of the suspensions prepared at different times and minor differences in the process of forming the nanographite films. Figure 3 also shows the capacitance values for multiple batches of electrodes prepared over a time period of several months. Although Figure 3 shows some overlap in the capacitance ranges for the different types of electrodes due to a higher variation in capacitance between different batches, there is the same trend of the capacitances in the order [K+valinomycin]·TPFPB < TDDMA·NO<sub>3</sub> < TBA·TPFPB < K·TPFPB as also shown in Table 1.

The effect of an additional electrolyte on the capacitance was assessed using the same chronopotentiometry method for ISE membranes doped with 10 mmol/kg TDDMA·NO<sub>3</sub> only and for membranes doped with 10 mmol/kg TDDMA·NO<sub>3</sub> and 10 mmol/kg ETH500 (electrodes prepared on the same day with the same nanographite suspension; see Table 2). Although the capacitances of these two sets of electrodes are close, addition of ETH500 increases the capacitance of TDDMA·NO<sub>3</sub> electrodes within a 95% confidence interval. As evident from Figure 1, theory predicts a capacitance increase by ~25% with addition of this concentration of ETH500, while the experimental result is an increase by ~24%. Increases in capacitance with ionic strength should be taken into account when comparing data for solid-contact ISEs with membranes differing in ionic strength.

**Table 2.** Average capacitance determined with  $\pm 500$ ,  $\pm 100$ , and  $\pm 50$  nA currents for electrodes with nanographite solid contacts and plasticized PVC membranes containing TDDMA·NO<sub>3</sub>, and TDDMA·NO<sub>3</sub> with ETH500 (prepared on the same day with the same nanographite suspension).

current (nA)	capacitance (mF)	specific capacitance (F/g)
TDDMA·NO <sub>3</sub>		
500	0.50±0.03	2.5±0.2
100	0.51±0.06	2.5±0.3
50	0.49±0.04	2.5±0.2
$TDDMA\cdot NO_3 + ETH500$		
500	0.61±0.08	3.0±0.4
100	0.61±0.06	3.1±0.3
50	0.64±0.09	3.2±0.4

In order to probe whether specific interactions of the ions with the nanographite affect the capacitance of devices with an overlying ion-selective membrane, the same experiments were performed with SWCNTs as solid-contact material. We note that the overall capacitance was slightly smaller with SWCNTs as compared to nanographite, which is explained by use of only half the mass of carbon applied per SWCNT-modified electrode as compared to the nanographite-based electrodes, and the two carbon types having quite different specific surface areas per weight. Therefore, we refer here to specific capacitance, computed as capacitance per g of carbon material.

For both types of solid contact, the specific capacitance depends on the composition of the ISE membrane. As shown in Figure 2, the specific capacitance increased in the order [K+valinomycin]·TPFPB < TDDMA·NO<sub>3</sub> < K·TPFPB when using SWCNTs as the solid contact, the same as for nanographite solid contacts. Interestingly, the specific capacitance ranges from 1.5 to 3.5 F/g for various ions with SWCNTs, while for nanographite the specific capacitance ranges from 1.2 to 5.2 F/g. Thus, the difference in capacitance between electrodes with and without valinomycin is larger in magnitude when using nanographite as compared to SWCNTs. A likely reason for this is the presence of internal surfaces in nanographite that exhibit size exclusion effects, while SWCNTs have only external surfaces.

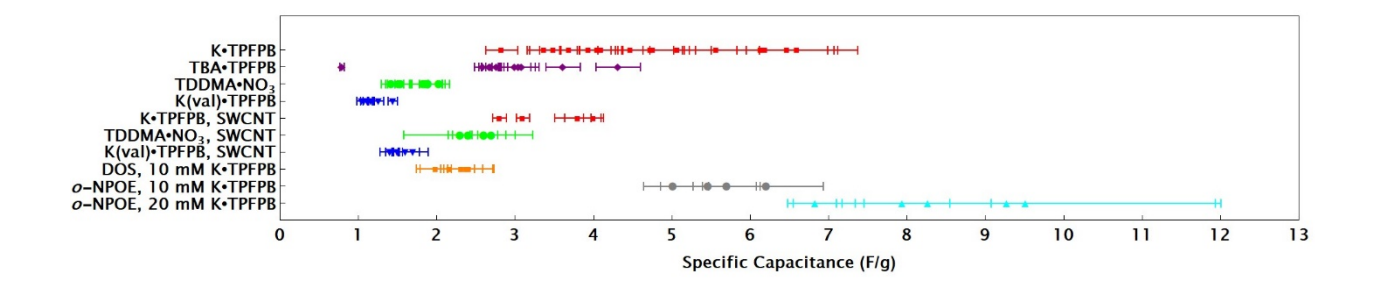


**Figure 2.** Specific capacitance values of nanographite (upper four data sets) and SWCNT (middle three data sets) solid contacts with *o*-NPOE plasticized PVC membranes containing K·TPFPB, TDDMA·NO<sub>3</sub>, [K+valinomycin]·TPFPB, and TBA·TPFPB. The lower three data sets are for specific capacitance values of nanographite solid contacts and plasticized PVC membranes with various plasticizers and concentrations of K·TPFPB.

There is the possibility that the capacitances as determined here do not fully reflect the formation of an equilibrium electrical double-layer but are affected by the slow ion movement in the bulk of the ion-selective membranes. Indeed, it has been reported for chronopotentiometry with activated carbon electrodes that the experimentally measured capacitance decreased by 30% when the charging time was reduced thousandfold.<sup>64</sup> In a case like this, the experimentally determined capacitance is expected to depend on the electrical resistance of the electrolyte solution. This prompted us to assess the resistance of ISEs with nanographite solid contacts and overlying plasticized PVC membranes.

Resistance values are shown in Table S6, and a similar plot to Figure 2 showing the resistances of all electrodes across multiple experiments is presented in Figure S8. The resistance of these sensors is affected by the identity of the ions in the ISE membrane, as is expected due to differing ion mobilities in the membrane bulk. Because conductance is the inverse of resistance, it follows that the conductance of the ion-selective membranes falls in in the order

[K+valinomycin]·TPFPB < TDDMA·NO $_3$  < TBA·TPFPB < K·TPFPB, which is identical with the order of capacitances. However, while the capacitance for K·TPFPB was approximately four times the capacitance for [K+valinomycin]·TPFPB, the conductance for K·TPFPB is only about twice as large as for [K+valinomycin]·TPFPB. Clearly, differences in mobility of ions in the membrane bulk alone cannot explain the large differences in the measured capacitances. Indeed, the small capacitance changes when the applied current was increased tenfold suggest that effects of ion mobilities in the membrane bulk, if relevant at all, are comparatively small, especially at an applied current of  $\pm 50$  nA.

#### Effect of Membrane Polarity on Double-layer Capacitance

As discussed in the theory section above, the dielectric constant of the medium is an important factor in determining the capacitance, with smaller dielectric constants expected to result in smaller capacitance values (see Figure S2). Therefore, we also used as plasticizer both DOS and o-NPOE. Notably, maybe counter-intuitively, DOS with its lower dielectric constant ( $\varepsilon$ =3.9) is well known to interact more strongly with small cations such as K<sup>+</sup> and Ca<sup>2+</sup> than o-NPOE ( $\varepsilon$ =23.9), which can be explained by cation–dipole interactions to the carbonyl groups of DOS.<sup>65</sup>

Figure 2 shows a comparison of the capacitance of ISEs with nanographite solid contacts and sensing membranes containing 10 mM K·TPFPB as ionic site and DOS or *o*-NPOE as plasticizer. Using DOS results in a decrease in the capacitance by roughly 50% compared to membranes plasticized with *o*-NPOE, similar to the theoretically predicted decrease, which is ~70%. It can additionally be seen that with *o*-NPOE as plasticizer, increasing the K·TPFPB concentration results in a capacitance increase by a similar magnitude as theoretically predicted, that is, ~30%. Clearly, comparison of capacitance values for different carbon materials when

using different plasticizers or different ionic site concentrations is not meaningful unless these effects are considered. As shown in Figure 3 too, ISEs with larger capacitances generally have larger uncertainties associated with them. (For the resistance of these electrodes, see Figure S9.)

#### Secondary Effects of Ion Identity

It is somewhat surprising that the ion identity has such a large effect on the observed capacitance, as double layer theory does not predict that ion size is as influential on the capacitance when measured near the PZC. As Figure 1 shows, theory predicts only a difference of ~10% between ISEs with membranes doped with K·TPFPB or [K+valinomycin]·TPFPB. Several reasons that may be considered for this finding.

One explanation that might be considered is that the identity of the ions in the ISE membrane affects water uptake. Water uptake into an ISE membrane results in an increase in the dielectric constant and, therefore, a higher capacitance. However, it has been shown that higher concentrations of both ionic site and ionophore result in decreased water uptake into plasticized PVC membranes, <sup>66</sup> and that for more hydrophobic ionophores water uptake is smaller. <sup>67</sup> Therefore, one might suspect that less hydrophobic ions result in larger water uptake, and, consequently, higher dielectric constants, resulting in higher capacitances. This does not appear to be the case here, though, as suggested by the resistance and capacitance values of ISEs with membranes that contained TDDMA·Cl and Li·TPFPB. While the uptake of water into ISE membranes takes place over the course of ~24 h, neither the capacitance nor the resistance of TDDMA·Cl and Li·TPFPB electrodes changed significantly over a period of 20 h of conditioning in 10 mM LiCl (see Table S7). Ion-exchange does not take place in these systems because the exchangeable ion in the membranes of these ISEs is identical with the ion of the same charge sign in the conditioning solution. Therefore, water uptake is the only significant

process during conditioning. Although there is a slight decrease in capacitance of the Li·TPFPB electrodes over time, it is clear that, even with no conditioning, the capacitance of the Li·TPFPB electrodes is much higher than that of TDDMA·Cl electrodes. This suggests that differences in water uptake cannot explain the majority of the capacitance differences observed here.

An alternative explanation for the large effect on ion size on capacitance relates to the ion size itself. For smaller ions, one might suspect that there is a larger accessible surface area in a porous solid contact. Indeed, optimization of the ion size relative to the pore size has been shown to result in increased capacitance for electrical double-layer capacitors (although ion sizes in the latter case are typically substantially smaller). 68-69 This would perhaps be expected to result in a difference between the capacitance measured on positive current application versus that measured on negative current application, which at least near the open circuit potential was not observed in this work. Moreover, DFT analysis of the  $N_2$  sorption isotherm shows that  $\approx 7\%$  of the pore volume and  $\approx 26\%$  of the pore surface area in nanographite pertains to pores with diameters of 2 nm or smaller, suggesting that under full equilibrium conditions the surface areas accessible to smaller ions is not much larger than for bigger ions. It seems rather unlikely, though, that full equilibration of the electrical double layer is reached over the short time period of the 10 s current pulses, as they are illustrated in Figure S7. Instead, the pore structure of nanographite may hinder over a short timeframe the access of ions to smaller pores, which may be followed over a longer time period by charge redistribution into the entire pore system. Similar kinetic limitations of ion transport into meso- and microporous carbon materials have been reported in the field of electrostatic capacitors. <sup>70,71</sup> It appears quite possible that smaller ions, in addition to being able to access a somewhat larger surface area than larger ions, also

penetrate the porous nanographite layer more quickly than larger ions, but this effect is not necessarily directly related to mobilities in the membrane bulk.

Lastly, as mentioned above in the discussion of the theory of the double-layer capacitance, it is possible that specific interactions between the ions in the sensing membrane and the nanographite (or SWCNTs) surface affect the capacitance in a wide range of potentials relative to the PZC.<sup>72</sup> This could result in the OCP arising at a point that does not correspond to the PZC.

#### **Conclusions**

Chronopotentiometry experiments show that the capacitance of solid-contact ISEs is affected substantially by the identity of the ions in the sensing membrane. Both the cation and the anion matter, with larger ions generally resulting in smaller capacitances. As predicted by double-layer theory, a higher concentration of ions in the membrane results in increased capacitance, be that whether a highly lipophilic electrolyte is added into the ISE membrane or whether the concentration of the ionic sites is increased. Also, as confirmed by variation of the plasticizer, the capacitance increases with the polarity of the membrane matrix. This demonstrates that comparison of relatively small differences in capacitance of ISEs with different solid-contact materials is not meaningful if the identity and concentration of the membrane ions and the membrane polarity are ignored.

Interestingly, the largest effect of ions on the capacitance of membranes as measured with chronopotentiometry is likely not an effect of ion size on the maximum ion concentration in the double layer, since these measurements are taken near the OCP (see the section on double-layer theory). This effect is still poorly understood but may be related to charge redistribution within the high surface-area carbon layer, which is too slow to occur on the time scale of a typical

chronopotentiometry experiment. Also, for high surface-area carbons with many micropores, the

accessible area is likely different for ions of different sizes.

We note that comparisons are made more difficult by the vastly different electrode sizes

and thicknesses of the transducer layer that have been reported in the literature. Often, when ion-

selective electrodes are developed for a specific application, the capacitance is assessed using the

electrode construction (i.e., plasticizer, ions present in the membrane) most desirable for the

application. While this value will in fact be most relevant to the device's specific use, it is not

necessarily the most useful value to compare different types of solid contacts. For the latter

purpose, reporting of capacitance per weight of solid-contact material is recommended.<sup>4</sup>

Moreover, in particular for high-surface-area solid-contact materials, the batch-to-batch

variability of the capacitance can significantly exceed in-batch variability. This should also be

considered when comparing different devices.

**Associated Content** 

Supporting Information

The Supporting Information contains further experimental details, the BET sorption isotherm of

nanographite, model predictions of the effect of the solvent dielectric constant on the

capacitance, chronopotentiograms as well as capacitance and resistance values for different

electrodes, the equivalent circuit model used to fit impedance data, and a description of the

model used to predict the effect of membrane properties on capacitances.

**Author Information** 

Corresponding Author

Philippe Bühlmann; orcid.org/0000-0001-9302-4674; Email: <u>buhlmann@umn.edu</u>

20

Authors

Celeste R. Rousseau; orcid.org/0000-0002-5418-4525

Yevedzo E. Chipangura; orcid.org/0000-0002-5185-2049

Andreas Stein; orcid.org/0000-0001-8576-0727

### **Notes**

The authors declare the following competing financial interests.

### Acknowledgments

This work was funded by the National Science Foundation Grant CHE-1710024 and CHE-2203752. C.R.R. acknowledges an NSF-GRFP and a Kenneth E. and Marion S. Owens Endowed Fellowship (Univ. Minnesota). We thank Emily E. A. Robinson for thoughtful suggestions on the manuscript.

#### References

- 1. Lindner, E.; Gyurcsanyi, R. E., Quality control criteria for solid-contact, solvent polymeric membrane ion-selective electrodes. *J. Solid State Electrochem.* **2009**, *13* (1), 51-68.
- 2. Hu, J. B.; Stein, A.; Bühlmann, P., Rational design of all-solid-state ion-selective electrodes and reference electrodes. *TrAC, Trends Anal. Chem.* **2016**, *76*, 102-114.
- 3. Zdrachek, E.; Bakker, E., Potentiometric sensing. *Anal. Chem.* **2019**, *91* (1), 2-26.
- 4. Rousseau, C. R.; Bühlmann, P., Calibration-free potentiometric sensing with solid-contact ion-selective electrodes. *TrAC, Trends Anal. Chem.* **2021,** *140*, 116277.
- 5. Bobacka, J.; Ivaska, A.; Lewenstam, A., Potentiometric ion sensors. *Chem. Rev.* **2008**, *108* (2), 329-351.
- 6. Bobacka, J.; McCarrick, M.; Lewenstam, A.; Ivaska, A., All-solid-state poly(vinyl chloride) membrane ion-selective electrodes with poly(3-octylthiophene) solid internal contact. *Analyst* **1994**, *119* (9), 1985-1991.
- 7. Kisiel, A.; Marcisz, H.; Michalska, A.; Maksymiuk, K., All-solid-state reference electrodes based on conducting polymers. *Analyst* **2005**, *130* (12), 1655-1662.
- 8. Lindfors, T.; Ivaska, A., Stability of the inner polyaniline solid contact layer in all-solid-state K<sup>+</sup>-selective electrodes based on plasticized poly(vinyl chloride). *Anal. Chem.* **2004,** *76* (15), 4387-4394.
- 9. Bobacka, J., Potential stability of all-solid-state ion-selective electrodes using conducting polymers as ion-to-electron transducers. *Anal. Chem.* **1999,** *71* (21), 4932-4937.
- 10. Papp, S.; Bojtar, M.; Gyurcsanyi, R. E.; Lindfors, T., Potential reproducibility of potassium-selective electrodes having perfluorinated alkanoate side chain functionalized poly(3,4-ethylenedioxytiophene) as a hydrophobic solid contact. *Anal. Chem.* **2019**, *91* (14), 9111-9118.
- 11. Sjoberg-Eerola, P.; Nylund, J.; Bobacka, J.; Lewenstam, A.; Ivaska, A., Soluble semiconducting poly(3-octylthiophene) as a solid-contact material in all-solid-state chloride sensors. *Sens. Actuators B, Chem.* **2008**, *134* (2), 878-886.
- 12. Lindfors, T., Light sensitivity and potential stability of electrically conducting polymers commonly used in solid contact ion-selective electrodes. *J. Solid State Electrochem.* **2009,** *13* (1), 77-89.
- 13. Gyurcsanyi, R. E.; Nyback, A. S.; Toth, K.; Nagy, G.; Ivaska, A., Novel polypyrrole based all-solid-state potassium-selective microelectrodes. *Analyst* **1998**, *123* (6), 1339-1344.
- 14. He, N.; Papp, S.; Lindfors, T.; Hofler, L.; Latonen, R. M.; Gyurcsanyi, R. E., Prepolarized hydrophobic conducting polymer solid-contact ion selective electrodes with improved potential reproducibility. *Anal. Chem.* **2017**, *89* (4), 2598-2605.
- 15. Zou, X. U.; Cheong, J. H.; Taitt, B. J.; Bühlmann, P., Solid contact ion-selective electrodes with a well-controlled Co(II)/Co(III) redox buffer layer. *Anal. Chem.* **2013**, *85* (19), 9350-9355.
- 16. Zou, X. U.; Zhen, X. V.; Cheong, J. H.; Bühlmann, P., Calibration-free ionophore-based ion-selective electrodes with a Co(II)/Co(III) redox couple-based solid contact. *Anal. Chem.* **2014**, *86* (17), 8687-8692.
- 17. Mendecki, L.; Mirica, K. A., Conductive metal-organic frameworks as ion-to-electron transducers in potentiometric sensors. *ACS Appl. Mater. Interfaces* **2018**, *10* (22), 19248-19257.

- 18. Klink, S.; Ishige, Y.; Schuhmann, W., Prussian blue analogues: A versatile framework for solid-contact ion-selective electrodes with tunable potentials. *ChemElectroChem.* **2017**, *4* (3), 490-494.
- 19. Lai, C.-Z.; Fierke, M. A.; Stein, A.; Bühlmann, P., Ion-selective electrodes with three-dimensionally ordered macroporous carbon as the solid contact. *Anal. Chem.* **2007,** *79* (12), 4621-4626.
- 20. Fierke, M. A.; Lai, C.-Z.; Bühlmann, P.; Stein, A., Effects of architecture and surface chemistry of three-dimensionally ordered macroporous carbon solid contacts on performance of ion-selective electrodes. *Anal. Chem.* **2010**, *82* (2), 680-688.
- 21. Hu, J.; Zou, X. U.; Stein, A.; Bühlmann, P., Ion-selective electrodes with colloid-imprinted mesoporous carbon as solid contact. *Anal. Chem.* **2014**, *86* (14), 7111-7118.
- 22. Zhang, T.; Lai, C.-Z.; Fierke, M. A.; Stein, A.; Bühlmann, P., Advantages and limitations of reference electrodes with an ionic liquid junction and three-dimensionally ordered macroporous carbon as solid contact. *Anal. Chem.* **2012**, *84* (18), 7771-7778.
- 23. Rius-Ruiz, F. X.; Crespo, G. A.; Bejarano-Nosas, D.; Blondeau, P.; Riu, J.; Rius, F. X., Potentiometric strip cell based on carbon nanotubes as transducer layer: Toward low-cost decentralized measurements. *Anal. Chem.* **2011**, *83* (22), 8810-8815.
- 24. Crespo, G. A.; Macho, S.; Xavier Rius, F., Ion-selective electrodes using carbon nanotubes as ion-to-electron transducers. *Anal. Chem.* **2008**, *80* (4), 1316-1322.
- 25. Crespo, G. A.; Gugsa, D.; Macho, S.; Rius, F. X., Solid-contact pH-selective electrode using multi-walled carbon nanotubes. *Anal. Bioanal. Chem.* **2009**, *395* (7), 2371-2376.
- 26. Yang, C. L.; Chai, Y. Q.; Yuan, R.; Guo, J. X.; Jia, F., Ligand-modified multi-walled carbon nanotubes for potentiometric detection of silver. *Anal. Sci.* **2012**, *28* (3), 275-282.
- 27. Yuan, D. J.; Anthis, A. H. C.; Afshar, M. G.; Pankratova, N.; Cuartero, M.; Crespo, G. A.; Bakker, E., All-solid-state potentiometric sensors with a multiwalled carbon nanotube inner transducing layer for anion detection in environmental samples. *Anal. Chem.* **2015**, *87* (17), 8640-8645.
- 28. Papp, S.; Kozma, J.; Lindfors, T.; Gyurcsanyi, R. E., Lipophilic multi-walled carbon nanotube-based solid contact potassium ion-selective electrodes with reproducible standard potentials. A comparative study. *Electroanalysis* **2020**, *32* (4), 867-873.
- 29. Li, F.; Ye, J.; Zhou, M.; Gan, S.; Zhang, Q.; Han, D.; Niu, L., All-solid-state potassium-selective electrode using graphene as the solid contact. *Analyst* **2012**, *137* (3), 618-623.
- 30. Jaworska, E.; Lewandowski, W.; Mieczkowski, J.; Maksymiuk, K.; Michalska, A., Critical assessment of graphene as ion-to-electron transducer for all-solid-state potentiometric sensors. *Talanta* **2012**, *97*, 414-419.
- 31. Hernandez, R.; Riu, J.; Bobacka, J.; Valles, C.; Jimenez, P.; Benito, A. M.; Maser, W. K.; Xavier Rius, F., Reduced graphene oxide films as solid transducers in potentiometric all-solid-state ion-selective electrodes. *J. Phys. Chem. C* **2012**, *116* (42), 22570-22578.
- 32. Ping, J. F.; Wang, Y. X.; Ying, Y. B.; Wu, J., Application of electrochemically reduced graphene oxide on screen-printed ion-selective electrode. *Anal. Chem.* **2012**, *84* (7), 3473-3479.
- 33. Paczosa-Bator, B., All-solid-state selective electrodes using carbon black. *Talanta* **2012**, *93*, 424-427.
- 34. Paczosa-Bator, B.; Piech, R.; Cabaj, L., The influence of an intermediate layer on the composition stability of a polymeric ion-selective membrane. *Electrochim. Acta* **2012**, *85*, 104-109.

- 35. Fouskaki, M.; Chaniotakis, N., Fullerene-based electrochemical buffer layer for ion-selective electrodes. *Analyst* **2008**, *133* (8), 1072-1075.
- 36. Zhao, L. J.; Jiang, Y.; Wei, H.; Jiang, Y. A.; Ma, W. J.; Zheng, W.; Cao, A. M.; Mao, L. Q., In vivo measurement of calcium ion with solid-state ion-selective electrode by using shelled hollow carbon nanospheres as a transducing layer. *Anal. Chem.* **2019**, *91* (7), 4421-4428.
- 37. Jiang, C. M.; Yao, Y.; Cai, Y. L.; Ping, J. F., All-solid-state potentiometric sensor using single-walled carbon nanohorns as transducer. *Sens. Actuators B, Chem.* **2019**, *283*, 284-289.
- 38. Mattinen, U.; Rabiej, S.; Lewenstam, A.; Bobacka, J., Impedance study of the ion-to-electron transduction process for carbon cloth as solid-contact material in potentiometric ion sensors. *Electroanalysis* **2011**, *56* (28), 10683-10687.
- 39. Crespo, G. A.; Macho, S.; Bobacka, J.; Rius, F. X., Transduction mechanism of carbon nanotubes in solid-contact ion-selective electrodes. *Anal. Chem.* **2009**, *81* (2), 676-681.
- 40. Anderson, E. L.; Bühlmann, P., Electrochemical impedance spectroscopy of ion-selective membranes: Artifacts in two-, three-, and four-electrode measurements. *Anal. Chem.* **2016**, *88* (19), 9738-9745.
- 41. Toth, K.; Graf, E.; Horvai, G.; Pungor, E.; Buck, R. P., Plasticized polyvinyl-chloride) properties and characteristics of valinomycin electrodes. Low-frequency, surface-rate, and warburg impedance characteristics. *Anal. Chem.* **1986**, *58* (13), 2741-2744.
- 42. Nahir, T. M.; Buck, R. P., Steady-state-current impedance spectroscopy of plasticized pvc membranes containing neutral ion carriers. *Electrochim. Acta* **1993**, *38* (18), 2691-2697.
- 43. Zdrachek, E.; Bakker, E., Ion-to-electron capacitance of single-walled carbon nanotube layers before and after ion-selective membrane deposition. *Microchim. Acta* **2021**, *188* (5), 149.
- 44. Wardak, C.; Pietrzak, K.; Morawska, K.; Grabarczyk, M., Ion-selective electrodes with solid contact based on composite materials: A review. *Sensors* **2023**, *23* (13), 5839.
- 45. Ding, J. W.; Qin, W., Recent advances in potentiometric biosensors. *TrAC, Trends Anal. Chem.* **2020**, *124*.
- 46. Bakker, E.; Bühlmann, P.; Pretsch, E., Carrier-based ion-selective electrodes and bulk optodes. 1. General characteristics. *Chem. Rev.* **1997**, *97* (8), 3083-3132.
- 47. <a href="https://www.graphitestore.com/gs-4827-nano-graphite-powder">https://www.graphitestore.com/gs-4827-nano-graphite-powder</a>.
- 48. Bard, A.; Faulkner, L., *Electrochemical methods: Fundamentals and applications*. 2 ed.; John Wiley and Sons: Hoboken, NJ, USA, 2000.
- 49. Biesheuvel, P. M.; van Soestbergen, M., Counterion volume effects in mixed electrical double layers. *J. Colloid Interface Sci.* **2007**, *316* (2), 490-499.
- 50. Hatlo, M. M.; van Roij, R.; Lue, L., The electric double layer at high surface potentials: The influence of excess ion polarizability. *Europhys. Lett.* **2012**, *97* (2), 28010.
- 51. Wang, H.; Pilon, L., Accurate simulations of electric double layer capacitance of ultramicroelectrodes. *J. Phys. Chem. C* **2011**, *115* (33), 16711-16719.
- 52. Bikerman, J. J., Structure and capacity of electrical double layer. *Philos. Mag.* **1942**, *33* (220), 384-397.
- 53. Han, Y. N.; Huang, S. H.; Yan, T. Y., A mean-field theory on the differential capacitance of asymmetric ionic liquid electrolytes. *J. Phys. Condens. Matter* **2014**, *26* (28).
- 54. Zhang, Y.; Huang, J., Treatment of ion-size asymmetry in lattice-gas models for electrical double layer. *J. Phys. Chem. C* **2018**, *122* (50), 28652-28664.
- 55. Uematsu, Y.; Netz, R. R.; Bonthuis, D. J., The effects of ion adsorption on the potential of zero charge and the differential capacitance of charged aqueous interfaces. *J. Phys. Condens. Matter* **2018**, *30* (6), 064002.

- 56. Para, G.; Jarek, E.; Warszynski, P., The Hofmeister series effect in adsorption of cationic surfactants—theoretical description and experimental results. *Adv. Colloid Interface Sci.* **2006**, *122* (1), 39-55.
- 57. Żubrowska, M.; Wróblewski, W.; Wojciechowski, K., The effect of lipophilic salts on surface charge in polymeric ion-selective electrodes. *Electrochim. Acta* **2011**, *56* (17), 6114-6122.
- 58. Yajima, S.; Tohda, K.; Bühlmann, P.; Umezawa, Y., Donnan exclusion failure of neutral ionophore-based ion-selective electrodes studied by optical second-harmonic generation. *Anal. Chem.* **1997**, *69* (10), 1919-1924.
- 59. Dong, X. I. N.; Spindler, B. D.; Kim, M.; Stein, A.; Bühlmann, P., Spontaneous mesoporosity-driven sequestration of ionic liquids from silicone-based reference electrode membranes. *ACS Sens.* **2023**, *8* (4), 1774-1781.
- 60. Eugster, R.; Rosatzin, T.; Rusterholz, B.; Aebersold, B.; Pedrazza, U.; Rüegg, D.; Schmid, A.; Spichiger, U. E.; Simon, W., Plasticizers for liquid polymeric membranes of ion-selective chemical sensors. *Anal. Chim. Acta* **1994**, *289* (1), 1-13.
- 61. Choi, K. R.; Chen, X. V.; Hu, J.; Bühlmann, P., Solid-contact ph sensor with covalent attachment of ionophores and ionic sites to a poly(decyl methacrylate) matrix. *Anal. Chem.* **2021**, *93* (50), 16899-16905.
- 62. Choi, K. R.; Troudt, B. K.; Bühlmann, P., Ion-selective electrodes with sensing membranes covalently attached to both the inert polymer substrate and conductive carbon contact. *Angew. Chem. Int. Ed. Engl.* **2023**, *62* (28), e202304674.
- 63. Panella, B.; Hirscher, M.; Roth, S., Hydrogen adsorption in different carbon nanostructures. *Carbon* **2005**, *43* (10), 2209-2214.
- 64. Zuliani, J. E.; Caguiat, J. N.; Kirk, D. W.; Jia, C. Q., Considerations for consistent characterization of electrochemical double-layer capacitor performance. *J. Power Sources* **2015**, *290*, 136-143.
- 65. Bakker, E.; Xu, A. P.; Pretsch, E., Optimum composition of neutral carrier based ph electrodes. *Anal. Chim. Acta* **1994**, *295* (3), 253-262.
- 66. Lindfors, T.; Sundfors, F.; Hofler, L.; Gyurcsanyi, R. E., FTIR-ATR study of water uptake and diffusion through ion-selective membranes based on plasticized poly(vinyl chloride). *Electroanalysis* **2009**, *21* (17-18), 1914-1922.
- 67. He, N.; Lindfors, T., Determination of water uptake of polymeric ion-selective membranes with the coulometric Karl Fischer and FT-IR-attenuated total reflection techniques. *Anal. Chem.* **2013**, *85* (2), 1006-1012.
- 68. Largeot, C.; Portet, C.; Chmiola, J.; Taberna, P.-L.; Gogotsi, Y.; Simon, P., Relation between the ion size and pore size for an electric double-layer capacitor. *J. Am. Chem. Soc.* **2008**, *130* (9), 2730-2731.
- 69. Lin, R.; Taberna, P. L.; Chmiola, J.; Guay, D.; Gogotsi, Y.; Simon, P., Microelectrode study of pore size, ion size, and solvent effects on the charge/discharge behavior of microporous carbons for electrical double-layer capacitors. *J. Electrochem. Soc.* **2009**, *156* (1), A7.
- 70. Lewandowski, A.; Jakobczyk, P.; Galinski, M.; Biegun, M., Self-discharge of electrochemical double layer capacitors. *Phys. Chem. Chem. Phys.* **2013**, *15* (22), 8692-8699.
- 71. Ike, I. S.; Sigalas, I.; Iyuke, S., Understanding performance limitation and suppression of leakage current or self-discharge in electrochemical capacitors: A review. *Phys. Chem. Chem. Phys.* **2016**, *18* (2), 661-680.

72. Grahame, D. C., The electrical double layer and the theory of electrocapillarity. *Chem. Rev.* **1947**, *41* (3), 441-501.

# **TOC Figure**

